

Atomic and molecular clusters : Review of the studies

Kotake, Susumu
Division of Functional Properties Faculty of Engineering Tokyo University

<https://doi.org/10.15017/6591>

出版情報 : 九州大学機能物質科学研究所報告. 5 (1), pp.33-62, 1991-09-30. 九州大学機能物質科学研究所
バージョン :
権利関係 :

Atomic and molecular clusters: Review of the studies

Susumu KOTAKE*

Due to their interesting features of chemical and physical properties, remarkable progress has been made in the study of atomic and molecular clusters in these few years by using highly advanced techniques of experiment and computation. The studies reported span the range of cluster size from dimer to hundreds for understanding their formation mechanism, molecular structures, and chemical and physical properties. Here, these studies are reviewed to overview the present state-of-study.

1. INTRODUCTION

Clusters consisting of atoms or molecules of tens to hundreds are a new class of compounds, 'atomic or molecular clusters'. These clusters are expected to have very interesting chemical and physical properties that span the range from molecular to bulk. Of these clusters, the theoretical and experimental studies have had a very fast growth during the last few years. The interest in clusters stems from many sources. Small clusters have been found very useful in the study of intermolecular forces as well as physical and chemical dynamics of molecular collisions and energy transfer. Large clusters have been studied for understanding the early stages of nucleation and condensation, catalysis chemistry and transition phenomena between molecular and condensed bulk materials. Using the newly developed experimental techniques such as laser optics, spectrometry and cluster beams as well as highly powerful computers of high speed and large memory, extensive studies on the physical and chemical features of these clusters have been started in wide ranges of cluster sizes and species.

In addition, these clusters are expected to have many possibilities in engineering applications such as high energy beams, very fine particles and films, and mass separation. Work is also started on such applications of the molecular clusters for engineering problems.

In this article, the state-of-study of atomic and molecular clusters is reviewed, especially concerning on the formation process of clusters, their molecular structures, and the features of electrical, magnetic, chemical and physical properties, as shown in Table 1 to Table 4 in

Received June 24, 1991

*) Guest Professor, Division of Functional Properties (Nov. 1987~March 1990)

which clusters are conveniently classified as

- rare-gas clusters: Table 1,
- atomic clusters: Table 2,
- molecular clusters: Table 3, and
- water clusters: Table 4.

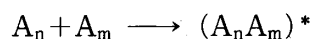
In these tables, the cluster species, the cluster size (the number of atoms or molecules), experimental (E) or computational (C) study, the main subjects of the study, and the experimental or computational method are presented for each study in References. References are cited especially from work reported in Journal of Chemical Physics because almost all studies of these clusters have been published in the journal.

2. CLUSTER FORMATION

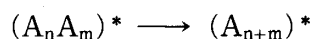
Much effort has been devoted to understanding the processes of cluster formation as the initial stages of nucleation and condensation as well as other dynamic processes of van der Waals molecules. From the standpoint of atomic and molecular collision dynamics, most of the dynamic behavior would be similar to that of ordinary chemical reactions. However, these clusters are weakly bound with dissociation energy usually two orders of magnitude smaller than normal chemical bonds. At the beginning of clustering, successive sticking of atoms or molecules may be the leading process, although coagulation and fragmentation of clusters become much more important as the density of clusters increases high enough.

Three ways can be considered as the formation process of clusters:

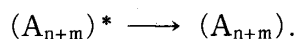
- (1) the atomic or molecular collision to make unbound coupling states of atoms or molecules;



- (2) the stabilization of the unbound states to make quasi-bound states of cluster;



- (3) the stabilization of the quasi-bound states to make bound states of cluster;



The stabilization of bound states from the higher energy level to the lower requires the extraction of energy from the complex or the redistribution of energy throughout the complex. The former may be associated with single or successive collisions of a third-body atom or molecule.

After clusters are formed, each collision between clusters and/or monomers is associated with the transfer of kinetic energy and leads to dissociation of these clusters as well as association with the same order of probability for the small clusters. The formation process of cluster is competition between these association and dissociation. During the process, thus, clusters never have the physical features of the equilibrium state, having a much smaller

number of bonds than the most compact configuration. The most compact configuration takes the greatest number of bonds with the minimum free energy. The growing clusters have the free energy larger than the minimum value because of their incompact configuration. More compact clusters are relatively more numerous in the low temperatures, where the surrounding heat bath has less kinetic energy which favors heat transfer of association rather than destructive collisions.

These clustering processes can be treated by the molecular dynamics method (MD) with newly available computers of high speed and large memory. The molecular dynamics method yields information about both static and dynamic behavior of the cluster system, by solving the equations of atomic or molecular motions with appropriate potentials. This method requires precise knowledge of intramolecular and intermolecular potentials in order to obtain quantitative information about the collision kinetics of cluster formation. In order to understand the fundamental dynamics of cluster formation, the quasi-classical trajectory method is also useful for simple and small cluster systems.

Clustering kinetics

In a system consisting of atom-atom, atom-molecule, molecule-molecule, molecule-cluster, or cluster-cluster reactant particles, employing an appropriate potential between them, the equations of motion of the particles can be solved as a function of the initial conditions of motion. Averaging of the initial conditions to get the same final state of motions or molecular configurations will give the reaction kinetics with corresponding reaction rates such as in chemical kinetics. This method is applied to simple systems, especially of rare gas molecules, because of their relatively well studied intermolecular potentials which may be expressed by a summation of pairwise potentials.

The statistical mechanism of reaction usually favors the more exothermic pathway. As the initial relative translational collision energy increases, the process of cluster formation shows nonstatistical behavior to give the product different from the more exothermic one, being dominated by the collision dynamics. On the exchange process of $A+BC$ system, the mechanism for reaction with the heavier atom (C) to form AC involves three-body interaction of "complex" formation (ABC^*) in which the product is randomly scattered. Because of the intermolecular interaction in the ABC^* complex, this process shows statistical behavior of exothermic reaction. As the collision energy increases, the abstraction of the lighter atom (B) by the incoming atom (A) to form AB occurs by a stripping mechanism in which the product molecule is scattered sharply in the forward direction of the reactant atom. The dissociation process of a cluster by monomer collision is greatly enhanced by the excitation of initial vibration and/or rotation.

In highly exothermic or endothermic reactions of covalently or ionically bonded clusters,

the rotational barrier exerts a negligible effect on the reaction dynamics. For clusters with lower bond energies, the rotational barrier is much of significance. The rotational barrier and potential minimum increases as the rotational state increases in the potential curve. At some rotational states (J_{\max}), the potential becomes strictly repulsive. All molecules having rotational states greater than J_{\max} should be dissociative. If the internal energy of the product is larger than the rotational barrier but less than the dissociation limit, the product may be rotationally metastable, playing an important role in the clustering process. When X and Y form a van der Waals bond, the processes of association $X+Y+M \longrightarrow XY+M$ and dissociation $XY+M \longrightarrow X+Y+M$ are markedly different from those for covalently bonded XY in the chemical processes.

Clustering by Molecular dynamics

Solving a set of dynamic equations of molecular motion with proper intramolecular and intermolecular potentials, the atomic and molecular motions can be obtained straightforward. It describes the coupling between intramolecular and intermolecular modes which induces energy transfer between those modes within the clusters as well as between the clusters. The coupling of intramolecular modes to intermolecular modes is relevant for predissociation of the cluster and energy redistribution in the cluster. In motions of the atomic nuclei, the electrons usually follow their ground state except for the case of metal where some of the electrons become delocalized from the atom.

In calculations of molecular dynamics, it is of the most importance to predict the intramolecular and intermolecular potentials. These potentials have been estimated empirically or semiempirically from the statistical data of thermal properties. But, the progress in computer power of high speed and large memory has made it possible to calculate the potentials directly by solving the Schrödinger equations of the atomic and molecular system with high-accuracy MO-LCAO (molecular orbital-linear combination of atomic orbitals) methods of configuration interaction self consistent field (CI SCF) with large number of orbital basis sets.

Clustering in supersonic free jets

For the clustering of gaseous species in experiments, supersonic free jets issued from a small aperture nozzle into high vacuum are commonly used. An isentropic expansion of the gas is associated with rapid decrease in the temperature which causes atomic or molecular clustering, relaxing the higher temperature state to the lower. The relaxation time can be related to the reaction-rate coefficients of the clustering collision kinetics, being a function of the pressure and temperature. Since the relaxation takes much more time as the pressure and temperature decrease, the relaxation process of expanding molecules would be frozen

essentially downstream parts of the flow. The frozen state occurs through a transition region along the jet axis. Upstream the region, the molecules are in a region of higher pressures and temperatures that the relaxation time is so small in comparison with the flow time that they are essentially in thermodynamic equilibrium. Until the gas reaches the freezing position, the mole fraction of clusters formed increases approximately in correspondence with local thermodynamic equilibrium, and the mole fraction is kept approximately constant downstream from this position. Thus, the terminal mole fraction of clusters formed is a function of the time history of the flow state through the transition region which controls the clustering kinetics.

3. PROPERTIES OF CLUSTERS

Since clusters are composed largely of surface atoms, their chemical and physical properties may well reflect the microscopic details of surface activity. Thus, they are expected to have physical and chemical properties that span the range from molecular to bulk. Questions of interest then arise;

- * How do the properties differ from the molecular or bulk ones?
- * Over what range of cluster size does the transition between molecular and bulk properties occur?
- * Do all physical and chemical properties make transition in the same range of cluster size?
- * Do all clusters behave similarly or do they show significant difference in the transition?

These interesting properties of cluster are molecular structures, electronic structures, electronic, vibrational and rotational states, chemical reactivities, and magnetic properties. For studying these properties, experimental and computational work has been conducted. Experimental studies firstly used the matrix method in which clusters were formed on a solid matrix, but recently employs the nozzle beam method (NB) in which clusters are produced in the process of supersonic expansion of gaseous atoms or molecules issued from a small aperture nozzle into vacuum. Atomic or molecular beams with clusters are then led to the measuring stage after being skimmed and collimated to measure the properties with optical, electronic and magnetic methods. These techniques include mass spectrometry, optical spectroscopy, electron spectroscopy, electron diffraction, and electron or photon ionization techniques.

For observing the cluster properties on computers, the Monte Carlo and molecular dynamics methods can be also used. Within statistical errors the results obtained by both methods are to be identical. For large volumes corresponding to small average density, the Monte Carlo method is more efficient since molecular dynamics takes more computer time to stabilize the temperature fluctuations due to evaporation and condensation. The molecular dynamics method gives the time evolution of the system which is essential in under-

standing the kinetic processes. Thus both methods are used to complement each other. In calculation of the stable cluster configurations in equilibrium by the molecular dynamics method, the total energy is constant and this gives rise to different metastable cluster distributions with different potential energy configurations for the same temperature. The equilibrium state corresponds to the lowest energy for a particular temperature and reaching this state can be a long process from uniform gas phase. The Monte Carlo method has the advantage that temperature remains fixed and the lowest energy state is obtained naturally, but has the disadvantage that time dependent properties cannot be studied.

Electronic structures

Understanding the changes in the electronic structure that occur in the transition from gas phase monomer to large clusters is critical to understanding nucleation and catalysis phenomena. There is very little information on electronic structures of large clusters, although there is a great deal of information available on dimers and small clusters. These electronic structures are mainly studied relating with ionization features of clusters. Properties pertaining to the process of direct ionization, autoionization and fragmentation have been widely studied by various techniques including

vacuum ultraviolet absorption spectroscopy,
electron impact method,
photoionization,
photoelectron spectroscopy,
photoionization resonance spectroscopy,
threshold photoelectron spectroscopy,
electronic emission spectroscopy, and
laser induced fluorescence.

Photoelectron spectroscopic methods are generally superior for the investigation of direct ionization process occurring at energies well above the initial thresholds. Photoionization mass spectrometry may be profitably applied to the measurement of transitions near the first ionization limit, appearance potentials for dissociative processes and autoionization peak positions.

As the photon spectroscopic techniques with lasers, various methods are employed;

- (1) Direct single photon ionization — direct measurement of ionization potentials and photoionization cross sections as the functions of wavelengths.
- (2) Resonant two-photon ionization — one photon excites the molecule to an electronically excited state and a second photon takes it to the ionized state to obtain information about the intermediate, excited electronic state and the excited state life time.
- (3) Photo-dissociation — excited molecules are dissociated and removed from the remain-

ing population.

- (4) Radiative repopulation — excited levels are repopulated into other lower electronic states by fluorescence which can be probed by a subsequent resonant two-photon ionization scan.

Nearly all of the early work on heavier clusters has been matrix isolation studies of metal clusters. These matrix studies of electronic transitions, Raman and resonance Raman effects, and electronic spin resonance can provide knowledge of the electronic structure of clusters. However, these studies are complicated

- (1) by guest-host and guest-guest interactions in the matrix, and
- (2) by the difficulty in spectroscopic assignment.

The latter arises in assigning spectroscopic features to a specific cluster in the distribution of clusters that are formed in the matrix. Questions always arise pertaining to the identity of the carrier of an observed spectroscopic transition, to the magnitude of the matrix-solute interactions, and to the observed details of rotational and vibrational structure in electronic transition.

From this reason, there has been an increasing amount of work on the electronic states of clusters in the gas phase of nozzle beam. Photoionization thresholds as a function of cluster size have been reported. In the studies of photoionization of clusters in the gas phase, two problems are to be considered;

- (1) contamination by fragmentation, and
- (2) true adiabatic threshold.

The contribution of fragmentation to the individual photoionization efficiency can be significant and be the dominant mechanism for production of lighter clusters. Thus, caution must be used in assigning features of a photoionization efficiency curve to autoionization structure of the neutral molecule of the same mass. For weakly bound clusters, the difference between the ground vibrational states of the neutral and the ions is very small for several tenths of a volt above the threshold. Thus, even though ions are formed near the adiabatic ionization threshold via autoionization of excited Rydberg states of the neutral, there is no guarantee that the true adiabatic threshold will be observed.

Ionization potentials

Studies of neutral clusters involve ionization, followed by analysis and detection of ionized clusters. Various features found in the cluster distributions are attributed to the structure of the neutral precursors. In such cases, attention has to be paid to the possibility of cluster fragmentation through the ionization. The validity of detected species through ionization related to the original distribution of the neutral clusters has been the subject of considerable debate and controversy, and is the critical problem to have information of

neutral clusters.

The general trend of ionization potential with cluster size follows decreasing as the cluster size increases from the atomic ionization potential to the bulk work function. But, for clusters especially pure metal clusters such as in the group Ia (Li, Na, K) and Ib (Cu, Ag, Au), odd/even alternation in ionization potential has been observed. In pure metal cluster systems, the effect is currently understood as a consequence of the odd/even alternation in the occupancy and energy of the highest occupied molecular orbital (HOMO). The even group Ia and Ib clusters are expected to have singlet ground states, whereas the odd clusters have doublet ground states with the unpaired electron in a fairly weakly bound HOMO. In the case of semiconductor clusters, this odd/even alternation in the electronic structure is not observed.

Sodium (Na) clusters yield ionization potentials of 4.9-4.0eV for $n=2-8$ (cf. 5.1eV for $n=1$ and 2.75eV for $n=\infty$). The odd/even alternation in ionization potentials can be observed evidently for $n < 6$ clusters.

Copper (Cu) clusters show pronounced odd/even alternation in ionization threshold, although all thresholds are less than the energy level of F_2 excimer laser of 7.9eV. This alternation behavior is also attributed to an odd/even alternation in the electronic structure of the copper clusters with the highest occupied molecular orbital (HOMO) of the even clusters being considerably more strongly bonding than it is in the clusters with an odd number of copper atoms.

Iron (Fe) clusters show the ionization potential decreasing in overall from the atomic ionization potential (7.9 eV) to the bulk work function (4.85 eV) as the cluster size increases. There are also clear oscillations in the 2-4 and 13-17 atom ranges. It may be evidence in support of the unique, nonbulklike electronic structure of small iron clusters.

Carbon (C) clusters have ionization potentials of 10-12eV which is very much higher than the work function of graphite (3.9-4.9eV). Clearly small carbon clusters are not bulk-like with respect to the ionization potential. This is a sign of the unique extended π bonding which characterizes the small carbon clusters. They show little odd/even alternation in the ionization potential.

Rare gas clusters do not follow a monotonous decrease of photoionization with cluster size due to the effects of fragmentation. A study of the Ar_3^+ photoionization efficiency curve as a function of nozzle stagnation pressure shows that the fragmentation of larger clusters can dominate the spectrum, even near threshold, and even when the nozzle conditions are such that the Ar_4^+ intensity is only a small fraction of the Ar_3^+ intensity. The Ar_3^+ photoionization efficiency curve, obtained using nozzle conditions such that no larger-cluster ions were detected, exhibits several broad peaks near threshold which show similarities to bands of the dimer. At high nozzle stagnation pressures, the photoionization efficiency

curves for Ar_n^+ ($n=2, 3$) are nearly identical due to the effects of fragmentation. These spectra exhibit two very broad features which are similar to those in the solid. Thus, for rare gas clusters, the effect of fragmentation is the most critical problem for measuring the ionization thresholds for each size cluster.

Molecular clusters have commonly the photoionization spectra of which the intense structure is rapidly decreased as the cluster size increases. Examination of threshold behavior shows ionization potentials of 11.80 ($n=2$), 11.72 ($n=3$), 11.66 ($n=4$), and 11.60 ($n=5$) eV for O_2 , and 13.32 ($n=2$), 13.24 ($n=3$), and 13.18 ($n=4$) eV for CO_2 . The difference between ionization potential of $(\text{O}_2)_{n-1}$ and $(\text{O}_2)_n$ gives a lower bound of the dissociation energy of $(\text{O}_2)_n^* \rightarrow (\text{O}_2)_{n-1}^* + \text{O}_2$. For $n=3, 4$, and 5 , the values obtained from experimental thresholds are 0.08, 0.06 and 0.06 eV, respectively, being relatively small. Those for CO_2 are 0.08 and 0.06 eV, respectively. This suggests that for these clusters, the binding is mainly electrostatic, in contrast to the chemical bonding in $(\text{O}_2)_2$.

Chemical reactivities

In neutral cluster reactions, it is difficult to unambiguously assign the reactants and products. The reactions of cluster ions reduces this ambiguity because it is possible to select a particular cluster size prior to reaction. Thus, almost all experiments of cluster reaction concern those of cluster ions produced in nozzle beams. The clusters are ionized by a high energy electron beam or laser before or after being skimmed. A specific cluster size is mass-selected by a quadrupole or other mass spectrometer, and then passed through a gas cell where reactant gas is introduced. At the end of the gas cell the products and unreacted ions are focused into a second mass spectrometer and mass-analyzed.

As such cluster reactions, O_2 , H_2 , D_2 , N_2 , Ar , Xe , H_2O and others are studied for the reaction with cluster ions of Ar , Al , Fe , alkali and metal elements. In the reactions between Al cluster ions and oxygen, the major products are Al_n^+ up to $n=13$ and no oxygen containing product ions were observed. On the contrary, in the reactions between Fe cluster ions and hydrogen, ion clusters show a strong size dependence in their reactivity, varying in their reaction rates with the cluster size n . The onset of bulk behavior does not occur gradually but appear to begin abruptly at $n=23$. The reaction rate increases abruptly from $n=8$ to take a peak value at $n=10-12$ and then decrease to a minimum at $n=17$, after which it increases again to a constant value at $n=23$.

Reactions metal clusters of iron, nickel, copper, and niobium ion clusters with low concentrations of D_2 , N_2 , and CO shows markedly different features for each metal. Dissociative chemisorption of D_2 is found to occur with dramatic sensitivity to cluster size in the case of iron, cobalt, and niobium clusters, with slight reactivity for nickel clusters, and with complete nonreactivity for copper clusters. Molecular nitrogen chemisorbs readily to

clusters of cobalt and niobium with reactivity pattern very similar to that observed with D_2 , but slightly to iron clusters. In contrary to the highly structured reactivity patterns of D_2 and N_2 , carbon monoxide shows only a slow monotonous increase in reactivity with cluster size.

Vibrational states

When clusters are held together by weak van der Waals attractive forces, even a single quantum of excitation in one of the vibrational modes of a molecule within the cluster is usually sufficient to cause prompt dissociation of the cluster. The gas-phase infrared absorption spectrum of such a cluster may thus be determined from measurements of the attenuation of the cluster population by an applied beam of infrared light.

Magnetic properties

Since clusters are composed of small number atoms or molecules, the total spin of cluster is reflected by the individual spin of the consisting particles. If the atom like aluminum is an odd-electron system, odd-atom clusters will have half-integer total spin and even-atom clusters have integer spin. The magnetic property is much different between odd-atom and even-atom clusters. This can be detected for nozzle beam clusters with the magnetic deflection method. The cluster beam is passed through a magnet before the detection of the mass spectrometry. The deflection of the cluster beam through the magnet is proportional to the magnetic moment of the cluster and the magnetic field gradient of the magnet, and inversely proportional to the mass or the number of atoms in the cluster. The spatial deflection pattern of cluster beam are measured to obtain the magnetic moment. The magnetic properties are examined relative to each other by comparing mass spectra by varying the magnetic field gradient which deflect the clusters on-axis. A general trend observed is that the magnetic moment per atom is reduced as the cluster size increases. The averaged magnetic moment of Al dimers is measured 3 to 4 times that of the bulk material and that of the trimer is 1 to 3 times.

Thermodynamic properties

At very low temperatures, clusters form crystallites with the molecular axes fixed in some orientation with respect to the crystallite body axes, being associated with only vibrational motions without rotational and translational modes. With increasing temperatures, these vibrational molecular fluctuations about this equilibrium orientation increase until, at some temperature, an orientational order-disorder transition takes place into a hindered rotor, plastic crystallite phase, being associated with rotational oscillations adding to vibrational motions. This is evidenced by an abrupt change in the slope of the energy-temperature curve. Until the crystallite melts, it is in the plastic crystallite phase, trans-

lationally ordered and rotationally disordered, with the molecules becoming nearly free rotors at the melting temperature. The orientational transition is also associated with a structural transition into a configuration nearly identical to those found for clusters of spherical atoms. Melting is accompanied by an abrupt change in slope of the energy and rms bond length function curves versus temperatures. After melting, finally at some temperature, the clusters dissociate, and thermodynamic properties never stabilize into well-defined values, where particles evaporate from the cluster and the cluster energy decreases toward zero.

The thermodynamic properties such as the internal energy, entropy and formation free energy can be calculated with the Monte Carlo method of the molecular dynamics method, although it is difficult to confirm them experimentally. Using the Monte Carlo method in the configuration space of the atoms in the cluster, ensemble averages of thermodynamic variables can be calculated. Generally, the average energy per particle as a function of temperature increases smoothly until a certain characteristic temperature of cluster size, at which point the slope of the curve (the specific heat) changes abruptly. This change is apparent only when the number of particles in the cluster exceeds about a certain value. The bond length distribution function, the number of bonds length (interparticle distances), shows at the lower temperatures the very well-resolved peak of a small half-width. When the temperature rises, the peaks begin to broaden, which means that a wider range of interparticle separations is being sampled. The maxima of the peaks also shift to larger values. While atoms in a solid usually move with small amplitudes about their equilibrium positions, liquid atoms have the freedom to move with much larger amplitudes within the body of the liquid. This greater freedom is reflected in the non-zero nature of the bond length distribution function in the between successive peaks. The mean square fluctuation in the bond lengths increases steadily almost linearly with temperature, until the melting temperature is reached where there is a sudden increase. The melting temperatures increase with increasing number of particles.

Phase-change temperature

The molecular dynamics study of CO₂ clusters having three translational and two orientational degrees of freedom with pair potential plus an electric quadrupole interaction show the temperature of orientational disorder, T_o , the temperature of rotational disorder (melting), T_m , and the temperature of translational disorder (dissociation), T_d as

size (n)	2	3	4	5	6	7	13	∞
T_o [k]	17.5	27.5	15	14	44	47.5	30	
T_m [k]		58	42	56	60	62.5	70	
T_d [k]	53	67.5	80	92	100	105	110	195

The general trends of the melting and dissociation temperature and the binding energy are to be increased with increasing the cluster size.

Formation free energy

For an Ar cluster of n atoms interacting with two-body additive Lennard-Jones potentials, a combination quantum mechanical Monte Carlo study shows that the free energy of formation rises very rapidly with cluster size and after taking the maximum decreases rapidly and that changes in the free energy with cluster size are associated with local minima to observe "magic" numbers at $n=7, 13, 19$. For other clusters, generally, the magic numbers are also observed by local minima in the free energy of formation of the clusters as a function of cluster size. The existence of magic numbers is usually very sensitive to conditions of temperature and pressure, and under some conditions is only observed in the quantum calculations. Much care should be taken of interpreting the magic numbers observed experimentally with the mass spectrometry of ionization, because the ionization process is much influenced by the cluster configuration as well as the cluster size.

Specific heat

The specific heat and the entropy are calculated if the energy is predicted as a function of the temperature. Generally, they increase rapidly and then gradually approach to the value of the bulk material as the cluster number increases. As each cluster passes through its melting temperature, they deviates considerably from the extension of solid state. There is a sudden increase in specific heat as the cluster melts.

4. STRUCTURES OF CLUSTERS

At sufficiently low temperatures, clusters may take some favorable structures influenced by the strong anisotropies in the intermolecular force with ordered motions of vibration and rotation. With increasing temperatures of the cluster, the anisotropies in the intermolecular force are reduced to average out due to orientational fluctuations and to make the effective interaction nearly spherically symmetric. The ordered structures are then relaxed to a configuration nearly identical to those found for clusters of spherical atoms such as rare gas crystallites.

Clusters interacting with a spherically symmetric pair potential may have the crystallite configuration such as

size (n):	configuration
3	equilateral triangle
4	tetrahedron
5	triangle bipyramid

- 6 octahedron
- 7 pentagonal bipyramid
- 13 icosahedron.

At these temperatures, the cluster is in the plastic crystallite phase, translationally ordered and rotationally disordered, but it takes statistically well-defined configurations corresponding to the temperature. Further increase in temperature results in melting and then dissociation of the cluster.

These are structures in statistically equilibrium in which clusters have sufficient time to equilibrate the intermolecular and intramolecular interactions of atomic and molecular motions. In this case, the configuration can be obtained by calculating the state of internal energy of the cluster under the interactions with the *ab initio* SCF method or other simplified methods to solve the relevant Schrödinger equations. The interaction energy of molecules consists of

- repulsion ($+r^{-12}$),
- dispersion ($-r^{-6}$),
- isolated charge densities, and
- induced multipoles.

The nonadditive terms of these contributions to the interaction energy of clusters exhibit a possible influence upon preferred molecular positions and orientations. These contributions can be predicted only by considering the complete higher-order interactions of cluster configurations, which takes considerably much time even with the fastest supercomputers. It seems likely, however, that a reasonably modified two-body potential, viewed as an effective pairwise potential, could favor the observed structures. With the Monte Carlo method using such a pairwise potential the equilibrium structures of clusters have been studied.

Static structures

In statistically equilibrium in which clusters can have sufficient relaxation time, the cluster structure should be the most stable so as to take the minimum of the internal energy. Thus, the static structure can be obtained by minimizing the internal energy of the cluster. For minimizing the intermolecular energy of a cluster with the Monte Carlo method, the energy for a particular configuration is calculated, then the configuration is changed by a step in one of the six (the three translational and three rotational) degrees of freedom and the energy is recalculated. If the resulting energy is lower, the step is repeated. If the energy is not lower, the configuration is stepped back to before and another degree of freedom is explored. A minimum energy configuration can thus be achieved. Care must be taken to start the cluster in number of sufficiently different configurations to ensure that all of the local minima in the potential surface of configuration are located.

For many substances such as rare gases, alkali metals, and semiconductors (but not transition metals), the abundance spectra of cluster size show local maxima at certain numbers. These numbers of the cluster size are in some cases independent of the method of ionization by which they are detected. These "magic" numbers are usually interpreted as corresponding to more stable than other clusters of similar size. For a few classes of materials, the principles determining cluster stability and the occurrence of magic numbers have been identified and many magic numbers have been predicted theoretically in this way.

For rare gases, the structure of the magic number is determined by geometric hard sphere packing. Since icosahedral packing is denser than close-packed structures, the magic numbers are the icosahedral structures at 13, 19, 55, 147 etc. For the free-electron-like alkali metals, the stable structure of the magic number clusters comes from a complete filling of a set of electron levels or a filling of electrons in one-electron levels corresponding to the self-consistent potential. They occur at 2, 8, 20, 40 etc. For partially ionic compound materials, the Coulomb interaction between the cations and anions can determine the structure with help of a point charge ionic model.

These stable structures of cluster ions can be measured by the Fourier transform ion cyclotron resonance method (FT-ICR). In the method, the ionized clusters are introduced in the region of a magnetic field which confines the ions into cyclotron motions mass-selected by the magnetic Lorentz force. During the cyclotron motions trapped in the region of the magnetic field, unstable clusters are removed due to dissociation and only stable clusters can be survived without any dissociation.

Dynamic structures

In the formation process of clusters, cluster structures may not always be of the static ones related to the corresponding condition in equilibrium. While these dynamic structures can be calculated with the molecular dynamics method, they can be also observed experimentally with the electron diffraction method. Due to their low proportion in comparison to the monomers, however, there is a certain limit below which the average size of clusters cannot be decreased without reducing noticeable electron diffraction patterns. Within this condition, the structure can be analyzed by comparing the experimental patterns with calculated diffraction patterns for assumed cluster models. Electron diffraction in the study of cluster structure has advantages over X-ray and neutron diffraction in resolving power which damps slowly with their intermolecular distance, less noise arising from counting statistics, and more structural information for amorphous materials.

Atomic clusters

Alkali metal clusters are of large interest because of some specific properties of the

chemical bond between alkali atoms which cannot be explained without taking into account the electronic correlation. Due to a relatively small number of electrons, which should be necessarily correlated, the elaborate quantum chemical method can be used. The *ab initio* CI calculations indicate a very high stability for the geometries with five-fold rotational symmetry axis such as pentagonal pyramidal ($n=6$), pentagonal bipyramidal ($n=7$), and icosahedron ($n=13$), suggesting the "magic" numbers of atoms frequently observed in experiments.

For Li_4 and Na_4 , the rhombic and bent square geometries are predicted by *ab initio* CI methods to be the most stable arrangement for the singlet and triplet states, respectively. More symmetrical planar square and tetrahedron ones are highly unstable due to their biradical features. However, nature of spin coupling strongly influences the stability of Li_4 and Na_4 geometrical arrangements. Different methods yield different configurations as the most favorable geometry; the linear chain (without polarizations), the square (the diatomics-inmolecular method), the tetrahedron (the $X\alpha$ method), and so on.

Atomic clusters of relatively larger number of electrons can be calculated by using all-electron and effective core potential methods. Such a calculation shows that for Be_{13} the face-centered structure is the lowest, and for Al_{13} the hexagonally close-packed structure is the lowest, while in the bulk metal Be and Mg have hexagonally close-packed structures and Al has a face-centered structure.

Group IVb elements (carbon, silicon, germanium, tin, and lead) appear to be particularly interesting for clusters. They condense into polyatomic aggregates, even in a vapor in thermal equilibrium with liquid or solid. In fact, carbon vapor at 2500 K contains more than 60% trimers. Their structure is not expected to resemble that of the corresponding crystals. These clusters take several close-packed structures corresponding to $n=13$ consisting of a central atom surrounded by a complete shell of outer atoms. An additional atom, which lies on the surface of such a highly symmetric compact core, could be expected to be weakly bonded.

Carbon clusters are interpreted as linear species involving alternating singlet and triplet ground states for odd- and even-numbered clusters. Within the given symmetry constraints at the Hartree-Fock level of theory, *ab initio* calculations can characterize the structures and energies of different isomers (linear and cyclic), including the effects of d-type polarization functions and electron correlation. Although the linear structures are more stable than the cyclic structures at the Hartree-Fock level, the effects of electron correlation yield that the ground state is the planar cyclic structure in an inplane distorted form of the symmetric benzene-like geometry. Thus, the cyclic rings may be more stable for larger systems.

In the experiment of these clusters produced by laser vaporization, the cluster distributions for $n=2-9$ depend strongly on the experimental conditions. In the $n=10-25$ range,

however, the magic numbers at 11, 15, 19, and 23 are identical for all the measurements on positive clusters, regardless whether they have been directly produced or a photoionization step was involved. Beyond $n=38$ only even clusters are seen and there is a broad maximum around $n=50-70$. Especially, the carbon cluster of $n=60$, C_{60} , is found to be an extremely stable one, having a closed, spheroidal graphitic structure of perfect truncated icosahedron like a soccerball made up of twenty surfaces of hexagons and pentagons.

Rare-gas clusters

The Lennard-Jones (6-12) pairwise potential gives four distinct geometric isomers for the cluster of $n=7$ of which the pentagonal geometry takes the minimum energy in the equilibrium configuration. From this structure of pentagonal bipyramid (BP), possible stable structures can be induced as

icosahedron (BP+1+BP; $n=13$),

double icosahedron (BP+5+BP; $n=19$),

dodecahedron (icosahedron+its faces (20); $n=33$) etc.

The electron diffraction work for small clusters produced in a free jet expansion clearly demonstrated the noncrystalline structure for $20 < n < 50$. This structure is identical to that of solid models constructed by a molecular dynamics calculation with Lennard-Jones potential; polyicosahedral geometry composing of icosahedra of 13 atoms which are either joined one to the other or interpenetrating each other ($n=13, 22, 28, 39, 42, 48, 65, 67, \dots$). However, as the cluster size increases above $n=50$, the polyicosahedral structure tends to turn into another more stable one. Multilayer icosahedral clusters are said to be one of these stable structures. Such icosahedra are made up of twenty identical tetrahedra possessing a common vertex and connected with each other through adjacent faces ($n=55, 147, 309, \dots$). Comparing the densitograms with calculated diffraction functions confirms the transition from the polyicosahedral structure to the multilayer icosahedral structure for clusters of about 50 atoms.

Molecular clusters

Molecular clusters have numerous variety of configurations of which the computational prediction is very difficult even for very simple small clusters such as dimers. Only for specified configurations, calculations are carried out with appropriate intra- and intermolecular potentials.

The CO_2 dimer has the lowest energy calculated with the configuration that the two molecules take a parallel orientation, each inclined at about 55 degrees to the intermolecular axis and separated by approximately 3.5 Å. The infrared spectrum of dimers in CO_2 dimers, however, has been interpreted as a T-shaped structure with a 4.1 Å between molecular

centers of mass. Carbon dioxide clusters, $(\text{CO}_2)_n$, formed in a free jet expansion ($n=10^2-10^5$) shows the cubic structure of the bulk material even when they contain less than some 10^2 molecules. Their high quadrupolar interaction may cause the cubic structure to be the most stable one, suggesting that carbon dioxide clusters consist of single microcrystals in contrast with Ar, C_6H_6 and others which show noncrystalline structures in small-sized clusters.

REFERENCES

The following are found in Journal of Chemical Physics.

Rare-gas clusters

- R7901 D.Frenkel and J.P.McTague, 70-6, 2695 (1979)
- R7902 D.E.Freeman, K.Yoshino & Y.Tanaka, 71-4, 1780 (1979)
- R7903 T.K.Lim, K.Duffy & S.Nakaichi, 70-10, 4782 (1979)
- R7904 R.A.Aziz, J.Presley & U.Buck, 70-10, 4737 (1979)
- R8101 H.Helm, K.Stephan & T.D.Mark, 74-7, 3844 (1981)
- R8102 T.M.Cooper and R.R.Birge, 74-10, 5669 (1981)
- R8103 P.A.Christiansen, K.S.Pitzer, Y.S.Lee et al., 75-11, 5410 (1981)
- R8201 P.M.Dehter and S.T.Pratt, 76-2, 843 (1982)
- R8202 P.M.Dehter, 76-3, 1263 (1982)
- R8203 S.T.Pratt and P.M.Dehter, 76-7, 3433 (1982)
- R8204 E.D.Poliakoff, P.M.Dehter & J.L.Dehter, 76-11, 5214 (1982)
- R8301 M.G.White and J.R.Grover, 79-9, 4124 (1983)
- R8302 J.Farges, M.F.De Feraudy, B.Rauolt & G.Torchet, 78-8, 5067 (1983)
- R8401 D.J.Trevor, J.E.Pollard & Y.T.Lee, 80-12, 6083 (1984)
- R8501 D.L.Freeman and J.D.Doll, 82-1, 462 (1985)
- R8601 J.Farges, M.F.De Feraudy, B.Rauolt & G.Torchet, 84-6, 3491 (1986)
- R8602 A.J.Stace, 85-10, 5774 (1986)
- R8603 U.Buck and H.Meyer, 84-9, 4854 (1986)
- R8604 F.G.Amar and R.S.Berry, 85-10, 5943 (1986)
- R8701 P.Scheier and T.D.Mark, 86-5, 3056 (1987)
- R8702 R.J.Shul, R.Passarella, B.L.Upschulte et al., 86-8, 4446 (1987)
- R8703 H.Janssens, W.Vanmarcke, E.Desoppere et al., 86-9, 4925 (1987)
- R8704 T.D.Klots, C.Chuang, R.S.Ruoff et al., 86-10, 5315 (1987)
- R8705 H.L.Davis, J.Jellinek & R.S.Berry, 86-11, 6456 (1987)
- R8706 T.L.Beck, J.Jellinek & R.S.Berry, 87-1, 545 (1987)
- R8707 O.Echt, M.C.Cook & A.W.Castleman, 87-6, 3276 (1987)
- R8708 S.Stringari and J.Treiner, 87-8, 5021 (1987)
- R8709 C.R.Albertoni, R.Kuhn, H.W.Sarkas & A.W.Castleman, 87-8, 5043 (1987)
- R8710 J.A.Northby, 87-10, 6166 (1987)
- R8801 M.Amarouche, G.Durand & J.P.Malrieu, 88-2, 1010 (1988)
- R8802 H.S.Gutowsky, C.Chuang, T.D.Klots et al., 88-5, 2919 (1988)
- R8803 T.L.Beck and R.S.Berry, 88-6, 3910 (1988)
- R8804 T.L.Beck, D.M.Leitner & R.S.Berry, 89-3, 1681 (1988)
- R8805 R.G.Lethbridge and A.J.Stace, 89-7, 4062 (1988)
- R8901 K.Norwood, J-H.Guo & C.Y.Ng, 90-6, 2995 (1989)
- R8902 K.Hiraoka and T.Mori, 90-12, 7143 (1989)
- R8903 W.Miehle, O.Kandler, T.Leisner & O.Echt, 91-10, 5940 (1989)

Atomic and Molecular Clusters

- R8904 P.G.Lethbridge and A.J.Stace, 91-12, 7685 (1989)
R8905 G.Gantefor, G.Broker, E.H-Krappe & A.Ding, 91-12, 7972 (1989)
R9001 G.Chalasiniski, M.M.Szczesniak & S.M.Cybulski, 92-4, 2481 (1990)
R9002 D.J.Wales and R.S.Berry, 92-7, 4283 (1990)
R9003 K.Hiraoka and T.Mori, 92-7, 4408 (1990)
R9004 Y.Mizukami and H.Nakatzuji, 92-10, 6084 (1990)
R9005 H.Buchenau, E.L.Knuth, J.Northby et al., 92-11, 6875 (1990)
R9006 R.J.Vos, J.H.van Lenthe & E.B.van Duijneveldt, 93-1, 643 (1990)
R9007 M.Kristensen and N.Bjerre, 93-2, 983 (1990)
R9008 Z.Y.Chen, C.D.Cogley, J.H.Hendrickes et al., 93-5, 3215 (1990)
R9009 P.S.Dardi and J.S.Dalher, 93-5, 3562 (1990)

Atomic clusters

- A7701 H.Komienne and R.I.Byer, 67-6, 2536 (1977)
A7702 M.Moskovits and J.E.Hulse, 67-9, 4271 (1977)
A7703 O.Navaro and W.Kolos, 67-11, 5066 (1977)
A7704 K.D.Jordan and J.Simons, 67-9, 4027 (1977)
A7705 L.S.Bartell, B.Rault & G.Torchet, 66-12, 5387 (1977)
A7706 W.J.Stevens and M.Kraus, 67-5, 1977 (1977)
A7801 D.O.Welch, O.W.Lazareth, G.J.Dienes & R.D.Hatcher, 68-5, 2159 (1978)
A7901 J.Berkwitz, C.H.Baston & G.L.Goodman, 71-6, 2624 (1979)
A7902 J.A.Beswick and J.Jorter, 71-11, 4737 (1979)
A8001 V.E.Bondybey and J.H.English, 73-1, 42 (1980)
A8002 T.Bergman and P.F.Liao, 72-2, 886 (1980)
A8003 J.H.Sinfelt and G.H.Via, 72-9, 4832 (1980)
A8004 T.P.Martin and H.Schaber, 73-8, 3541 (1980)
A8005 J.L.Gole, R.H.Childs, D.A.Dixon & R.A.Eades, 72-12, 6368 (1980)
A8006 H.O.Beckmann, J.Koutecky & V.B-Koutecky, 73-10, 5182 (1980)
A8007 H.Basch, M.D.Newton & J.W.Moskowitz, 73-9, 4492 (1980)
A8101 J.H.Sinfelt and G.H.Via, 75-11, 5527 (1981)
A8102 H.Figger, R.Strabinger & H.Walther, 75-1, 179 (1981)
A8103 T.G.Dietz, D.Duncan, D.E.Powers & R.E.Smalley, 74-11, 6511 (1981)
A8104 J.Demuynck, M.Rohmer, A.Strich & A.Veillard, 75-7, 3443 (1981)
A8105 R.A.Chiles, C.E.Dykstra & K.D.Jordan, 75-2, 1044 (1981)
A8106 L.Noodlemann, 74-10, 5737 (1981)
A8201 J.Gayda, P.Bertand & F.Theodule, 77-7, 3387 (1982)
A8202 G.A.Thompson and D.M.Lindsay, 74-2, 959 (1982)
A8203 G.Pacchioni and J.Koutecky, 77-11, 5850 (1982)
A8204 H.Tatewaki, E.Miyoshi & T.Nakamura, 76-10, 5073 (1982)
A8205 R.A.Eades, M.L.Hendewerk, R.Frey et al., 76-6, 3075 (1982)
A8301 G.A.Thompson, F.Tischler & D.M.Lindsay, 78-10, 5946 (1983)
A8302 K.I.Peterson, P.D.Dao & A.W.Castleman, 79-2, 777 (1983)
A8303 H.Figger and X.Zhu, 79-3, 1320 (1983)
A8304 D.E.Powers and R.E.Smalley, 78-6, 2866 (1983)
A8305 M.D.Morse and R.E.Smalley, 79-11, 5316 (1983)
A8306 J.B.Hopkins, P.R.L-Smith, M.D.Morse & R.E.Smalley, 78-4, 1627 (1984)
A8307 J.L.Martins, R.Car and J.Buttet, 78-9, 5646 (1983)
A8308 H.Partridge, D.P.Dixon et al., 79-4, 1859 (1983)
A8309 E.Miyoshi, H.Tatewaki & T.Nakamura, 78-2, 815 (1983)
A8401 K.I.Peterson, P.D.Dao, R.W.Farley & A.W.Castleman, 80-5, 1780 (1983)

- A8402 E.A.Rohlfing, D.M.Cox & A.Kaldor, 81-7, 3322 (1984)
 A8403 E.A.Rohlfing, D.M.Cox, A.Kaldor & K.H.Johnson, 81-9, 3846 (1984)
 A8404 T.P.Martin and A.Kakizaki, 80-9, 3956 (1984)
 A8405 M.D.Morse and R.E.Smalley, 80-11, 5400 (1984)
 A8406 W.Muller and W.Meyer, 80-7, 3311 (1984)
 A8407 D.A.Bishop and C.Pouchan, 80-2, 789 (1984)
 A8408 G.Pacchioni and J.Koutecky, 81-8, 3588 (1984)
 A8409 M.Tomonari, H.Tatewaki & T.Nakamura, 80-1, 344 (1984)
 A8501 T.P.Martin and H.Schaber, 83-2, 855 (1985)
 A8502 L.S.Zheng, P.J.Brucat & R.E.Smalley, 83-8, 4273 (1985)
 A8503 J.R.Heath and R.E.Smalley, 83-11, 5520 (1985)
 A8504 M.D.Morse, M.E.Geusic, J.R.Heath and R.E.Smalley, 83-5, 2293 (1985)
 A8505 S.Wang, 82-10, 4633 (1985)
 A8506 J.Diefenbach and T.P.Martin, 83-9, 4585 (1985)
 A8601 W.H.Crumley, J.S.Hayden & J.L.Gole, 84-10, 5250 (1986)
 A8602 J.C.Phillips, 85-9, 5246 (1986)
 A8603 D.M.Cox, D.J.Trevor et al., 84-8, 4651 (1986)
 A8604 M.F.Jarrold and J.E.Bower, 85-9, 5373 (1986)
 A8605 M.E.Geusic et al., 84-4, 2421 (1986)
 A8606 P.J.Brucat, L.S.Zheng & R.E.Smalley, 84-6, 3078 (1986)
 A8607 G.Igelmann, U.Wedig, P.Fuentealba & H.Stoll, 84-9, 5007 (1986)
 A8608 M.Tomonari, H.Tatewaki & T.Nakamura, 85-5, 2875 (1986)
 A8609 S.Walch and B.C.Laskowski, 84-5, 2734 (1986)
 A8610 K.Raghavachari, 84-10, 5672 (1986)
 A8611 K.Raghavachari, R.A.Whiteside & J.A.Pople, 85-11, 6623 (1986)
 A8612 J.Rubio, F.Illas & J.M.Ricart, 84-6, 3311 (1986)
 A8613 C.W.Bauschlicher and L.G.M.Petterson, 84-4, 2226 (1986)
 A8701 S.W.McElvany, B.I.Dunlap & A.O'Keefe, 86-2, 715 (1987)
 A8702 N.J.Kirchner and M.T.Bowers, 86-3, 1301 (1987)
 A8703 M.E.Geusic, M.F.Jarrold, T.J.McIlrath et al., 86-7, 3862 (1987)
 A8704 M.F.Jarrold, J.E.Bower & J.S.Kraus, 86-7, 3876 (1987)
 A8705 P.V.Madhavan and M.D.Newton, 86-7, 4030 (1987)
 A8706 W.D.Reents, A.M.Mujisce, V.E.Bondybey & M.L.Mandich, 86-10, 5568 (1987)
 A8707 C.W.Bauschlicher and S.R.Langhoff, 86-10, 5603 (1987)
 A8708 T.H.Upton, 86-12, 7054 (1987)
 A8709 C.Brechignac, P.Cahuzac & J.R.Poux, 87-1, 229 (1987)
 A8710 L.Hanley, S.A.Ruatta & S.L.Anderson, 87-1, 260 (1987)
 A8711 W.Forner and M.Seel, 87-1, 443 (1987)
 A8712 S.B.H.Bach, D.A.Garland, R.J.VanZee & W.Weltner, 87-2, 869 (1987)
 A8713 D.M.Lindsay, L.Chu, Y.Wang & T.F.George, 87-3, 1685 (1987)
 A8714 K.Raghavachari and J.S.Binkley, 87-4, 2191 (1987)
 A8715 L.G.M.Petterson and C.W.Bauschlicher, 87-4, 2205 (1987)
 A8716 C.W.Bauschlicher and L.G.M.Petterson, 87-4, 2198 (1987)
 A8717 W.Schulze, B.Winter & I.Goldenfeld, 87-4, 2402 (1987)
 A8718 K.LaiHing, R.G.Wheeler, W.L.Wilson & M.A.Duncan, 87-6, 3401 (1987)
 A8719 M.R.Zakin, D.M.Cox & K.Kalder, 87-8, 5046 (1987)
 A8720 C.Brechignac, P.Cahuzac, J-P.Roux et al., 87-10, 5694 (1987)
 A8721 M.F.Jarrold and J.E.Bower, 87-10, 5728 (1987)
 A8801 M.E.Geusic, R.R.Freeman & M.A.Duncan, 88-1, 163 (1988)
 A8802 D.M.Cox, K.C.Reichmann & A.Kaldor, 88-3, 1588 (1988)

Atomic and Molecular Clusters

- A8803 E.K.Parks, B.H.Weiller, P.S.Bechthold et al., 88-3, 1622 (1988)
A8804 Q.L.Zhang, Y.Liu, R.F.Curl, F.K.Tittel & R.E.Smalley, 88-3, 1670 (1988)
A8805 P.P.Radi, T.L.Bunn, P.R.Kemper et al., 88-4, 2809 (1988)
A8806 R.G.Wheeler, K.LaiHing, W.L.Wilson & M.A.Duncan 88-4, 2831 (1988)
A8807 C.Brechignac, P.Cahuzac & J.P.Roux, 88-5, 3022
A8808 Z.Fu, G.W.Lemire, Y.M.Hamrik et al., 88-6, 3524 (1988)
A8809 S.W.Buckner, J.R.Gord & B.S.Freiser, 88-6, 3678 (1988)
A8810 E.K.Parks, G.C.Nieman, L.G.Pobo & S.J.Riley, 88-10, 6260 (1988)
A8811 G.A.Antonio, B.P.Feuston, R.K.Kalia & P.Vashishta, 88-12, 7671 (1988)
A8812 M.E.Geusic and R.R.Freeman, 89-1, 223 (1988)
A8813 S.A.Ruatta and S.L.Anderson, 89-1, 273 (1988)
A8814 S.K.Cole and K.Liu, 89-2, 780 (1988)
A8815 K.Raghavachari and C.M.Rohlfing, 89-4, 2219 (1988)
A8816 S.McElvany, 89-4, 2063 (1988)
A8817 D.E.Bernholdt, D.H.Magers & R.J.Bartlett, 89-6, 3612 (1988)
A8818 M.M.Ross and S.W.McElvany, 89-8, 4821 (1988)
A8819 F.Spiegelmann and D.Pavolini, 89-8, 4954 (1988)
A8820 D.Houl, R.O.Jones, R.Car & M.Parrinello, 89-11, 6823 (1988)
A8901 M.Vala, T.M.Chandrasekhar, J.Szczepanski et al., 90-1, 595 (1989)
A8902 C.Brechignac, P.Cahuzac, J.Leygnier & J.Weiner, 90-3, 1492 (1989)
A8903 K.Raghavan, M.S.Stave & A.E.DePristo, 90-3, 1904 (1989)
A8904 J.M.L.Martin, J.P.Francois & R.Gijbels, 90-11, 6469 (1989)
A8905 V.Parasuk and J.Almlof, 91-2, 1137 (1989)
A8906 R.E.Leuchtner, A.C.Harms & A.W.Castleman, 91-4, 2753 (1989)
A8907 U.Ray, M.F.Jarrold, J.E.Bower & J.S.Kraus, 91-5, 2912 (1989)
A8908 B.H.Weiller, P.S.Bechthold, E.K.Parks et al., 91-8, 4714 (1989)
A8909 G.Durand, 91-10, 6225 (1989)
A9001 P.Fayet, A.Kalder & D.M.Cox, 92-1, 254 (1990)
A9002 T.J.Lee, A.P.Rendell & P.R.Taylor, 92-1, 489 (1990)
A9003 T.D.Klots, B.J.Winter, E.K.Parks & S.J.Riley, 92-3, 2110 (1990)
A9004 W.R.Creasy and J.T.Brenna, 92-4, 2269 (1990)
A9005 A.R.W.McKellar, 92-6, 3278 (1990)
A9006 P.P.Radi, M.T.Hsu, J.B-Lustig et al., 92-8, 4817 (1990)
A9007 D.L.Martin, L.M.Raff & D.L.Thompson, 92-9, 5311 (1990)
A9008 R.E.Leuchtner, A.C.Harms & A.W.Castleman, 92-11, 6527 (1990)
A9009 R.J.V.Zee and W.Weltner, 92-11, 6976 (1990)
A9010 A.P.Rendell, T.J.Lee & P.R.Taylor, 92-12, 7050 (1990)
A9011 W.R.Creasy, 92-12, 7223 (1990)
A9012 M.F.Jarrold, U.Ray & K.M.Creegan, 93-1, 224 (1990)
A9013 M.B.Knickelbein, S.Yang & S.J.Riley, 93-1, 94 (1990)
A9014 S.Yang and M.B.Knickelbein, 93-3, 1533 (1990)
A9015 V.B-Keuteckey, P.Fantucci & J.Keutecky, 93-6, 3802 (1990)
A9016 M.B.Knickelbein and S.Yang, 93-8, 5760 (1990)
A9017 K.Raghavachari, C.M.Rohlfing & J.S.Binkley, 93-8, 5862 (1990)
A9018 L.S.Wang, B.Niu, Y.T.Lee, D.A.Shirley et al., 93-9, 6310 (1990)
A9019 R.D.Kay, L.M.Raff & D.L.Thompson, 93-9, 6607 (1990)
A9020 T.J.Lee, A.P.Rendell & P.R.Taylor, 93-9, 6636 (1990)
A9021 T.T.Rantala, M.I.Stockman et al., 93-10, 7427 (1990)
A9022 C.W.Bauschlicher, S.R.Langhoff & H.Partridge, 93-11, 8133 (1990)
A9023 R.W.Hall, 93-11, 8211 (1990)

- A9024 J.R.Heath and R.J.Saykally, 93-11, 9392 (1990)
 A9025 Z.Fu, G.W.Lemire, G.A.Bishea & M.D.Morse, 93-12, 8420 (1990)
 A9026 W.Harbich, S.Fedrigo, F.Meyer et al., 93-12, 8535 (1990)
 A9027 C.Liang and H.F.Schaefer, 93-12, 8844 (1990)
 A9028 J.M.Martin, J.P.Francois & R.Gijbels, 93-12, 8850 (1990)
 A9029 J.D.Watts, I.Cernusak, J.Noga et al., 93-12, 8875 (1990)

Molecular clusters

- M7701 C.E.Klots and R.N.Compton, 67-4, 1779 (1977)
 M7702 J.Goodman and L.E.Brus, 67-10, 4408 (1977)
 M7801 G.Duquette et al., 68-6, 2544 (1978)
 M7901 A.R.Rossi and K.D.Jordan, 70-9, 4422 (1979)
 M7902 S.T.Ceyer and Y.T.Lee, 70-6, 2138 (1979)
 M7903 W.M.Trott, N.C.Blais & E.A.Walters, 71-4, 1692 (1979)
 M7904 W.L.Jorgensen, 71-12, 5034 (1979)
 M8001 S.L.Anderson, T.Hirooka & Y.T.Lee, 73-10, 4779 (1980)
 M8002 R.M.Berns and A.van der Avoird, 72-11, 6107 (1980)
 M8003 M.P.Casassa, D.S.Bomse et al., 72-12, 6805 (1980)
 M8004 Y.Ono, S.H.Linn, C.Y.Ng et al., 73-6, 2523 (1980)
 M8005 A.C.Leron et al., 73-1, 583 (1980)
 M8101 L.Jansen and R.Block, 75-2, 847 (1981)
 M8102 J.Erickson and C.Y.Ng, 75-4, 1650 (1981)
 M8103 P.D.Aldrich, A.C.Legon & W.H.Flygare, 75-5, 2126 (1981)
 M8104 S.H.Linn, Y.Ono & C.Y.Ng, 74-6, 3342 (1981)
 M8105 O.Novaro, S.Cruz & S.Castillo, 74-2, 1118 (1981)
 M8106 S.H.Linn and C.Y.Ng, 75-10, 4921 (1981)
 M8107 R.D.Etters, K.Flurchick & R.P.Pan, 75-2, 929 (1981)
 M8201 L.Schrivier and J.P.Perchard, 77-10, 4926 (1982)
 M8202 J.H.Futrell, K.Stephan & T.D.Mark, 76-12, 5893 (1982)
 M8203 K.Suzuki and K.Iguchi, 77-9, 4594 (1982)
 M8204 J.Tennyson and A.van der Avoird, 77-11, 5664 (1982)
 M8205 K.Stephan, T.D.Mark et al., 77-5, 2408 (1982)
 M8301 T.E.Gaough, M.Mengel, P.A.Rowntree & G.Scoles, 83-10, 4958 (1983)
 M8302 D.D.Nelson, G.T.Fraser & W.Klemperer, 83-12, 6201 (1983)
 M8303 G.D-Barrio and G.Albelda, 78-1, 280 (1983)
 M8304 J.Jortner, S.Leutwyler & Z.B-Yellin, 78-1, 309 (1983)
 M8305 R.K.Heenan, E.J.Valente & L.S.Bartell, 78-1, 243 (1983)
 M8306 F.Visser, R.E.S.Wormer & P.Stam, 79-10, 4973 (1983)
 M8307 M.P.Casassa, C.L.Western, F.G.Celii et al., 79-7, 3227 (1983)
 M8308 K.Hirao, 79-10, 5000 (1983)
 M8401 H.Kim, M.F.Jarrold & M.T.Bowers, 84-9, 4882 (1984)
 M8402 G.Torcht, H.Bouchier, J.Farges et al., 81-4, 2137 (1983)
 M8403 R.E.Miller, P.F.Vohral & R.O.Watts, 80-11, 5453 (1984)
 M8404 M.J.Howard, S.Burdenski & W.R.Gentry, 80-9, 4137 (1984)
 M8405 H.Z.Cao, E.M.Evleth & E.Kassab, 81-3, 1512 (1984)
 M8406 N.Ohasi and A.S.Pine, 81-1, 73 (1984)
 M8407 R.L.DeLeon and J.S.Muenter, 80-12, 6092 (1984)
 M8408 B.J.Howard, T.R.Dyke & W.Klemperer, 81-12, 5417 (1984)
 M8409 Z.Latajka and S.Scheiner, 81-1, 407 (1984)
 M8410 L.J.van de Burgt, J.Nicolai & M.C.Heaven, 81-12, 5514 (1984)

Atomic and Molecular Clusters

- M8411 G.Fitzgerald and H.F.Schaefer, 81-1, 362 (1984)
M8412 L.Sanche and M.Michaud, 81-1, 257 (1984)
M8501 K.J.Rensberger, R.A.Copeland et al., 83-3, 1132 (1984)
M8502 G.Fischer, R.E.Miller, P.F.Vohralik & R.O.Watts, 83-4, 1471 (1984)
M8503 H.Schinohara, N.Nishi & N.Washida, 83-4, 1939 (1985)
M8504 P.Brechignac, E.DeBenedictis et al., 83-5, 2064 (1985)
M8505 G.Fitzgerald, T.J.Lee & H.F.Schaefer, 83-12, 6275 (1985)
M8506 O.Echt, P.D.Dao, S.Morgan & A.W.Castleman, 82-9, 4076 (1985)
M8601 E.Knozlinger, H.Kollhoff & W.Langel, 85-9, 4881 (1986)
M8602 S.Liu, D.W.Michael, C.E.Dystra & J.M.Lisy, 84-9, 5032 (1986)
M8603 R.L.Redington and D.F.Hamill, 80-6, 2446 (1986)
M8604 S.Liu, C.E.Dykstre, K.Kolenbrander & J.M.Lisy, 85-4, 2077 (1986)
M8605 M.P.Casassa, J.C.Stephenson & D.S.King, 85-4, 2333
M8606 W.Kamke, B.Kamke, H.U.Kiefl & I.V.Hertel, 84-3, 1325 (1986)
M8607 P.C.Engelking, 85-5, 3103 (1986)
M8608 J.Nieman and R.Naaman, 84-7, 3825 (1986)
M8609 J.M.Lisy, 84-7, 4112 (1986)
M8610 U.Ross and T.Schulze, 85-5, 2664 (1986)
M8611 F.Carnovale, J.B.Peel & R.G.Rothwell, 85-11, 6261 (1986)
M8701 R.B.Frees, B.Dunlap, B.A.Waite & J.E.Campana, 86-3, 1276 (1987)
M8702 K.W.Jacks, Z.S.Huang, R.E.Miller & W.J.Lafferty, 86-8, 4341 (1987)
M8703 B.W.van de Waal, 86-10, 5660 (1987)
M8704 K.G.H.Baldwin and R.O.Watts, 87-2, 873 (1987)
M8705 P.C.Engelking, 87-2, 936 (1987)
M8706 H.D.Barth and F.Huisken, 87-5, 2549 (1987)
M8707 D.Scharf, J.Jortner & U.Landman, 87-5, 2716 (1987)
M8708 M.Tsukuda, N.Schima, S.Tsuneyuki et al., 87-7, 3927 (1987)
M8709 A.van der Avoird and G.Brocks, 87-9, 5346 (1987)
M8710 U.Buck, F.Huisken, C.Lauenstein et al., 87-11, 6276 (1987)
M8711 D.D.Nelson and W.Klemperer, 87-11, 6364 (1987)
M8801 F.Carnovale, J.B.Peel & R.G.Rothwell, 88-2, 642 (1988)
M8802 U.Buck and H.Meyer, 88-5, 3028 (1988)
M8803 J.P.Visticot, J.M.Mestdagh, C.Alcaraz et al., 88-5, 3081 (1988)
M8804 P.Scheier, A.Stamatovic & T.D.Mark, 88-7, 4289 (1987)
M8805 M.Gauthier, 88-9, 5439 (1988)
M8806 M.J.Deluca, B.Niu & M.A.Johnson, 88-9, 5857 (1988)
M8901 K.O.Bornsen, S.H.Lin, H.L.Selze & E.W.Schlag, 90-3, 1299 (1989)
M8902 G.Cardini, V.Schettino & M.L.Klein, 90-8, 4441 (1989)
M8903 C.Zhang, D.L.Freeman & J.D.Doll, 91-4, 2489 (1989)
M8904 A.C.Legon and A.P.Suckley, 91-8, 4440 (1989)
M8905 W.R.Peifer, M.T.Coolbaugh & J.F.Garvey, 91-11, 6684 (1989)
M9001 A.van der Pol, A.van der Avoird & P.E.S.Wormer, 92-12, 7498 (1990)
M9002 M.J.Deluca, C-C.Han & M.A.Johnson, 93-1, 268 (1990)
M9003 H.S.Gutowsky and C.Chuang, 93-2, 894 (1990)
M9004 M.M.Szczesniak, G.Chalasinski et al., 93-6, 4243 (1990)
M9005 P.Hobza, H.L.Selze & E.W.Schlag, 93-8, 5893 (1990)
M9006 R.S.Ruoff, T.Emilsson, C.Chuang et al., 93-9, 6363 (1990)

Water clusters

- W7601 O.Matsuoka, 64-4, 1351 (1976)

- W7701 T.R.Dyke, 66-2, 492 (1977)
W7702 T.R.Dyke, K.M.Mack & J.S.Muenter, 66-2, 498 (1977)
W7703 C.Y.Ng, D.J.Trevor & Y.T.Lee, 67-9, 4235 (1977)
W7901 M.van Hemet and A.van der Avoird, 71-12, 5310 (1979)
W8001 J.A.Odutola and T.R.Dyke, 72-9, 5062 (1980)
W8002 P.M.Holland and A.W.Castleman, 72-11, 5984 (1980)
W8003 Z.Slanina, 73-5, 2519 (1980)
W8004 A.B.Rakshit and P.Warneck, 73-10, 5074 (1980)
W8005 C.W.David, 73-10, 5395 (1980)
W8201 B.van Hensbergen, R.Block & L.Jansen, 76-6, 3161 (1982)
W8202 M.F.Vernon, D.J.Krajnovich & Y.T.Lee, 77-1, 47 (1982)
W8203 R.J.Beuhler and L.Friedman, 77-5, 2549 (1982)
W8301 R.C.Ward, B.N.Hale & S.Terazas, 78-1, 420 (1983)
W8302 A.E.Reed and F.Weinhold, 78-6, 4066 (1983)
W8303 B.A.Zilles and W.B.Person, 79-1, 65 (1983)
W8304 G.Torchet, P.Schwartz, J.Farges et al., 79-12, 6196 (1983)
W8401 B.K.Rao and N.R.Kestner, 80-4, 1587 (1984)
W8402 L.A.Curtiss and C.L.Eisgruber, 80-5, 2022 (1984)
W8403 D.Belford and E.S.Campbel, 80-7, 3288 (1984)
W8404 H.Haberland, C.Ludewigt et al., 81-8, 3742 (1984)
W8501 D.F.Coker, R.E.Miller & R.O.Watts, 82-8, 3554 (1985)
W8502 U.C.Singh and P.A.Kollman, 83-8, 4033 (1985)
W8601 M.J.Frisch, J.E.DelBene, J.Binkey & H.F.Schaefer, 84-4, 2279 (1986)
W8602 H.Shinohara, N.Nishi & N.Washida, 84-10, 5561 (1986)
W8603 M.M.Szczesniak and S.Scheiner, 84-11, 6328 (1986)
W8604 M.J.Wojcik and S.A.Rice, 84-6, 3042 (1986)
W8605 U.Nagashima, H.Shinohara & N.Nishi, 84-1, 209 (1986)
W8701 A.Engdahl and B.Nelander, 86-4, 1819 (1987)
W8702 S.Wuelfert, D.Harren & S.Leutwyler, 86-6, 3751 (1987)
W8703 A.Engdahl and B.Nelander, 86-9, 4831 (1987)
W8704 D.Belford and E.S.Campbell, 86-12, 7013 (1987)
W8705 P.L.M.Plummer and T.S.Chen, 86-12, 7149 (1987)
W8706 S.H.S.Salk and C.K.Lutrus, 87-1, 636 (1987)
W8707 L.H.Coudert, F.J.Lovas et al., 87-11, 6290 (1987)
W8708 E.Honegger and S.Leutwyler, 88-4, 2582 (1987)
W8709 R.N.Barnett, U.Landman, C.L.Cleveland & J.Jortner, 88-7, 4429 (1987)
W8801 B.Nelander, 88-8, 5245 (1988)
W8802 K.Hermansson, 89-4, 2149 (1988)
W8803 R.N.Barnett, U.Landman & A.Nitzan, 89-4, 2242 (1988)
W8804 K.Szalewicz, S.J.Cole, W.Kolos & R.Bartett, 89-6, 3662 (1988)
W8805 J.A.Kerr and J.Kiefer, 89-7, 4313 (1988)
W8806 L.A.Posey and M.A.Johnson, 89-8, 4807 (1988)
W8807 M.P.C.M.Krijn and D.Feil, 89-9, 5787 (1988)
W8901 T.Inoue and S.Kotake, 91-1, 162 (1989)
W8902 Z.S.Haung and R.E.Miller, 91-11, 6613 (1989)
W9001 O.Hess, M.Caffarell, C.Huiszoon & P.Claverie, 92-10, 6049 (1990)
W9002 R.N.Barnett, U.Landman, G.Makov & A.Nitzen, 93-9, 6226 (1990)

Atomic and Molecular Clusters

Table 1 Rare-gas clusters

Type	Size	E/C	Subjects	Methods	Ref
Ar	2	C	Raman spectra	classical methods	R7901
Ar	2	E	rot. spectra	discharge excited	R7902
Ne-Xe	4>	C	binding energy	pair potential	R7903
ArKr		C	transport properties	potential	R7904
NeXe, ArXe		E	double ionization	NB (nozzle beam)	R8101
Ar	17>	C	dispersive interaction	long-range force	R8102
Ar, Kr, Xe	2	C	effective potential	CISCF	R8103
Ar	6>	E	photoionization	NB	R8201
Ar	2	E	photoionization	NB	R8202
HeXe, ArXe		E	photoionization	NB	R8203
Xe	3>	E	photoionization	NB	R8204
Ar, Kr	3>	E	photoionization	NB, synchrotron	R8301
Ar	20-50	E	structure	NB, E-diffraction	R8302
Ne	2	E	photoionization	NB	R8401
Ar	n	C	thermal properties	MC (Monte Carlo)	R8501
Ar	50-750	E	structure	NB, E-diffraction	R8601
Ar	5-24	E	decomposition energy	NB	R8602
Ar	4-6	E	fragmentation	NB, He-cross beam	R8603
Ar	7	C	melting, isomers	MD (molecular dynam.)	R8604
Ar ⁺⁺	400<	E	double charged	NB	R8701
Ar ⁺	2	E	reaction (N ₂ , H ₂ , Xe)	NB, flow tube	R8702
Kr*	2	C/E	excimer formation, decay	rate eq., VUV	R8703
Ar	2	E	-HCl, -Cl cluster, rot. state	NB, MW	R8704
Ar	13	C	melting, freezing	MD	R8705
LJ	7-33	C	phase-change	MD	R8706
Kr	2	E	2 photon absorption	NB, dye laser	R8707
He	30>	C	properties, structure	density functional	R8708
Ar ⁺	3	E	photodissociation	NB, dye laser	R8709
LJ	13-147	C	structure, binding	MD	R8710
Xe	9, 13, 19	C	structure, stability	model Hamiltonian	R8801
Ar	4	E	-H cluster, rot. state	NB, MW	R8802
LJ	7-33	C	dynamics, structure	MD	R8803
Ar	3	C	phase change	G-P method	R8804
Ar ⁺	30-200	E	unimolecular fragmentation	NB, VG ZAB-E MS	R8805
Ar	2-4	E	photo-ion, electron spectra	NB	R8901
Ar ⁺	n	E	formation, stability	NB	R8902
Ar, Kr, Xe	n	E	icosahedral structure	NB	R8903
Kr ⁺	n	C	structure, properties	SCF	R8904
rg	n	E	photoionization	NB	R8905
Ar	3, 4	C	E-structure	MPSCF	R9001
Ar	n	C	melting, freezing	MD	R9002
rg	n	E	stability	NB	R9003
Ar	2	C	potential	CISCF	R9004
He	n	E	size distribution	NB	R9005
He	2	C	interaction energy	CISCF	R9006
He	2	C	structure	CISCF	R9007
Kr ⁺	n	E	photodissociation	NB	R9008
Ar, Mg	2	C	formation	rate eq.	R9009

note: rg: rare gas, LJ: Lennard-Jones gas, alk.: alkali, hal.: halogen,
 E: experimental work, C: computational work,
 E-: electronic, IE: ionization energy, IP: ionization potential,
 IR: infrared, FIR: far infrared, MW: micro-wave, PI: photo-ionization
 NB: nozzle beam, OB: oven beam, EB: electron beam,
 MD: molecular dynamics method, MC: Monte Carlo method,
 SCF: self consistent field method, CI: configuration interaction.

Table 2 Atomic clusters

Type	Size	E/C	Subjects	Methods	Ref.
Hg	2	E	fluorescence	OB (oven beam)	A7701
Cu	5>	E	vib. structures	LiF matrix, heated	A7702
Be	5>	C	interaction energy	SCF	A7703
Be	4>	C	E-affinity, stability	SCF	A7704
Ag	135>	C	E-scattering	wave theory	A7705
Mg	2	C	E-structure	MC, SCF	A7706
alk. hal.	44>	C	geometry, formation, vib.	simple shell theory	A7801
Li hal.	2	E	ionization potential	OB	A7901
hal	2	C	vib. dissociation	MD	A7902
Bi	2, 4	E	E-structure, absorp.	NeAr matrix, laser	A8001
Sr	2	E	photoassociation, potential	OB, laser	A8002
RuCu	n	E	structure	Si matrix, X-ray	A8003
Cu•hal.	3	E	FIR absorp.	OB, Si matrix	A8004
Li	3	C	E-structure, E-affinity	CISCF	A8005
Li, Na	4	C	structure	CISCF	A8006
Ni	6>	C	E-structure, binding energy	ECP-SCF	A8007
OsCu	n	E	structure	Si matrix, X-ray	A8101
Na	2	E	O reaction	cross beam	A8102
Al	3>	E	laser vaporization	NB (nozzle beam)	A8103
Cu	8, 6	C	E-structure, binding energy	SCF	A8104
Mg	4	C	binding energy	SCEP, CEPA	A8105
trn. metal	2	C	spin interaction	HFSCF	A8106
Fe	n	E	Magnetic properties	Mössbauer, matrix	A8201
K	3	E	E-structure	ESR, Ar matrix	A8202
Mg, Ca	2	C	structure	MRD-CISCF	A8203
Cu	6>	C	E-structure, binding energy	CISCF	A8204
Li, Na, K	3	C	E-affinity, vib.	SCF	A8205
Na, K	7	E	structure	ESR, Ar matrix	A8301
Na	2	E	reaction, photoionization	coaxial beams	A8302
alk.	2	E	O ₂ reaction, dissociation	cross beams	A8303
Cu	29>	E	photoionization	NB, laser	A8304
Cu	3	E	vib. structure, IE	NB, laser	A8305
Mo	25>	E	bond length, IE	NB, laser	A8306
Li, Na, K	3	C	E-structure, structure	PP-LSD	A8307
Ma, K, Rb	2	C	E-affinity	CISCF	A8308
Cu	3>	C	E-structure	SCF	A8309
Na	8>	E	photoionization, binding E.	NB	A8401
C	190>	E	size distribution	NB, laser PI	A8402
Fe	20>	E	photoionization	NB, laser PI	A8403
Cu•hal.	20>	E	size distribution	OB	A8404
Ni	2	E	E-structure	Nb, laser	A8405
Li, Na, K	2	C	E-structure	CISCF	A8406
Li	2	C	polarization	PP-CISCF	A8407
Li	13	C	stability, structure	MRD-CISCF	A8408
Zn	6>	C	E-level distribution	SCF	A8409
Si, Ge, Sn	50>	E	size distribution	OB	A8501
Nb ⁺ , Nb ⁻	n	E	size distribution	NB, laser	A8502
Si, Ge	n	E	fragmentation, E-structure	NB, laser	A8503

Atomic and Molecular Clusters

Table 2 Atomic clusters (continued)

Type	Size	E/C	Subjects	Methods	Ref.
Nb, Co, Cu, Ni, Fe	n	E	reaction (H ₂ , CO, N ₂)	NB, laser, cell	A8504
Cu	3>	C	structure, E-structure, IE	PP-SIC	A8505
alk. hal.	18>	C	structure	potential	A8506
Cu	3	E	E-structure	OB, laser	A8601
Ge, Si ⁺	n	C	structure	potential	A8602
Al	25>	E	magnetic properties	NB, mag. deflection	A8603
Al	25>	E	O ₂ reaction	NB, cell	A8604
C	20>	E	photo-fragmentation	NB, laser	A8605
Fe, Ni, Nb	n	E	photo-dissociation	NB, laser	A8606
alk.	2	C	dipole moment, IE	SEPPCI	A8607
Ni	6>	C	E-structure	CISCF	A8608
Cu	3	C	potential	CISCF	A8609
Si	20>	C	structure, E-structure	HF	A8610
C	6	C	structure	HFSCF	A8611
Be	7>	C	structure	CISCF	A8612
Be, Al, Mg	13	C	structure	CISCF	A8613
C ⁺	3-19	E	reaction (D ₂ , O ₂)	NB, FTMS	A8701
H ⁺	4, 6, 8, 10	E	size distribution	drift tube	A8702
C ⁺	3-20	E	photodissociation	NB, 248, 351nm	A8703
Al ⁺	3-26	E	collision-dissociation	NB, cell	A8704
Cu	2, 3, 5	C	reaction (O), O adsorption	CISCF	A8705
Si ⁺	2-6	E	reaction (XeF ₂)	cell	A8706
CuX _n	2	C	X=Li, Na, K, Be, Al, bonding	CISCF	A8707
Al	2-6	C	E-structure	drop model, CISCF	A8708
Kn	80>	E	photoionization	NB, Nd: YAG laser	A8709
Al ⁺	2-7	E	collision dissociation (Xe)	NB, cell	A8710
Li	2, 6	C	correlation energy, structure	CISCF	A8711
Ag	7	E	structure	Ne matrix, ESR	A8712
alk ⁻	3-8	C	stable structure	Hückel MO	A8713
C	2-10	C	structure, stability, frag.	CISCF	A8714
Al	2-6, 13	C	structure, stability	CISCF	A8715
Al	2-4	C	structure, stability	CISCF	A8716
Ge ⁺	4-46	E	stability	gas aggregation	A8717
Sn, Pb	25>	E	photoionization, size dist.	NB, excimer	A8718
Ta	11>	E	reaction (O)	O doped Ta	A8719
alk.	10>	E	adiabatic decomposition	NB, PI	A8720
Al ⁺	3-26	E	reaction (O)	NB, cell	A8721
Bi ⁺ , Sb ⁺	2-8	E	photoionization	NB, 248nm	A8801
C	60	E	size distribution	NB, excimer	A8802
Fe	13-23	E	reaction (H ₂ , NH ₃ , H ₂ O)	NB	A8803
Si ⁺ , Ge ⁺ , GaAs ⁺	40>	E	photoionization	NB, UV	A8804
C ⁺	60>	E	size distribution	NB, excimer	A8805
Sn, Bi, Pb, Sb, As	n	E	size distribution	NB, excimer	A8806
Kn ⁺	3-41	E	photodissociation	NB, UV, tandem TOF	A8807
Al	3	E	vib. states	NB, excimer	A8808
Zn ⁺ , Ag ⁺	5>	E	formation from oxide	laser desorption	A8809
Fe	n	E	reaction (NH ₃)	NB, flow tube	A8810
Ge	2-14	C	structure	potential MD	A8811

Table 2 Atomic clusters (continued)

Type	Size	E/C	Subjects	Methods	Ref.
Sb, Bi	20>	E	size distribution	NB, excimer	A8812
Al ⁺	2-19	E	reaction (O ₂ , N ₂ O)	sputtered, cell	A8813
Nb	7-12	E	photoionization	NB, excimer	A8814
Si	7-10	C	structure, vib. states	SCF	A8815
C ⁺	3-20	E	reaction (CH ₄ , C ₂ H ₂ , C ₂ H ₄)	NB, cell, FTICR	M8816
C	4	C	stability, E-properties	SCF	A8817
Sb ⁺ , Bi ⁺	n	E	formation, fragmentation	direct vaporized	A8818
Na, Na ⁺ , K, K ⁺	6>	C	E-structure	CISCF	A8819
S	13>	C	structure	E-density function	A8820
C	5	E	structure, IR spectra	NB	A8901
Na ⁺	n	C	unimolecular dissociation	SCF	A8902
Ni	n	E	structure, reaction (D ₂)	NB, cell	A8903
B, N	3>	C	structure, stability	CISCF	A8904
C	6	C	E-structure, structure	CISCF	A8905
Al ⁺	n	E	reaction (O)	NB, cell	A8906
Al ⁺	n	E	photodissociation	NB	A8907
Fe	n	E	reaction (H ₂ O)	NB, cell	A8908
Mg ⁺ , ⁺⁺	7>	E	structure, stability	NB	A8909
Pd	n	E	reaction (H ₂ , D ₂ , N ₂ , C ₂ H ₄ , C ₂ H ₆)	NB, cell	A9001
Be, Mg	3-5	C	structure, binding energy	SCF	A9002
Co	n	E	reaction (H), size dist.	NB, cell	A9003
C ⁺	n	E	formation	laser ablation	A9004
H ₂	2	E	IR spectra	NB	A9005
C ⁺	5-100	E	unimolecular dissociation	NB	A9006
Si	2	C	formation	MD	A9007
Cu ⁺	n	E	reaction (O)	NB, cell	A9008
Cu	7	C	structure	CISCF	A9009
Be	3, 4	E	vib. spectra	NB	A9010
C	n	E	cluster kinetics	rate eqs.	A9011
Ni	3-90	E	photodissociation	NB	A9012
Si	n	E	reaction (O)	NB, cell	A9013
Fe, CO	n	E	photoionization	NB	A9014
Na	3, 4, 8	C	photoelectron spectra	SCF	A9015
Si	n	E	photoionization	NB	A9016
S	n	E	structure, stability	NB	A9017
P ⁺ , As ⁺ , Sb ⁺	2, 4	C	photoelectron spectra	SCF	A9018
Si	4	C	formation	MD	A9019
Mg	n	C	vib. state	SCF	A9020
Si	n	C	E-structure	SCF	A9021
Cu, Ag, Au	4, 5	C	structure	SCF	A9022
Na	4-6	C	E-state	path integral	A9023
C	9	C	structure, vib. state	SCF	A9024
Al	2	E	E-state	NB	A9025
Ag	n	E	deposition (rare gas)	rare gas matrix	A9026
C	10	C	structure	CISCF	A9027
C	6-9	C	IR spectra	CISCF	A9028
Be	3	C	binding energy	SCF	A9029

Atomic and Molecular Clusters

Table 3 Molecular clusters

Type	Size	E/C	Subjects	Methods	Ref.
CO ₂	6>	E	E-affinity	NB (nozzle beam)	M7701
O ₂	2	E	vib. relaxation	NB, laser	M7702
NH ₃	2	C	potential	SCF	M7801
CO ₂	2	C	structure, IE	HF, SCF	M7901
C ₂ H ₄	n	E	photoionization	NB	M7902
CS ₂	2	E	photoionization	NB	M7903
CH ₃ OH	2	C	potential	SCF	M7904
H ₂ , O ₂	5>	E	photoionization	NB, laser	M8001
N ₂	2	C	structure	HF	M8002
C ₂ H ₄	2	E	IR spectra, dissociation	NB, CO ₂ laser	M8003
CS ₂	5>	E	photoionization	NB, UV	M8004
CO	2	E	rot. spectra	NB, MW	M8005
Cl ₂	2	C	structure, interaction E	perturb. E-theory	M8101
SO ₂	2	E	photoionization	NB	M8102
C ₂ H ₄ ·HCl		E	rot. structure	NB, MW	M8103
CO, N ₂ , NO	3>	E	photoionization	NB, UV	M8104
NH ₃	3	C	structure	SCF	M8105
CO ₂	4>	E	photoionization	NB, laser	M8106
CO ₂	13>	C	thermal properties, structure	MC	M8107
CH ₃ OH	2	E	IR spectra	Ar matrix	M8201
CO ₂ , NH ₃	2	E	collision dissociation	NB	M8202
C ₂ H ₄	2	C	potential, structure	exchange perturb.	M8203
N ₂	2	C	vib./rot. states	SCF	M8204
CO ₂	5>	E	ionization	NB	M8205
SF ₆	2	E	IR spectra	NB, CO ₂ -laser	M8301
NH ₃	2	E	IR spectra, rot. structure	NB, MW	M8302
He·I	2	C	vib. dissociation	MD	M8303
C ₆ H ₆ ·rg		C	structure	MC	M8304
C ₆ H ₆	n	E	structure	NB, E-diffraction	M8305
He, H, Ne, N ₂	2	C	intermol. correlation	CHF	M8306
C ₂ H ₄ ·HCl		E	vib. dissociation	NB, IR laser	M8307
CHO	2	C	energy, IP, E-affinity	cluster expan.	M8308
CO ₂	3	E	photo-dissociation	NB, laser	M8401
CO ₂	n	E	structure	NB, E-diffraction	M8402
C ₂ H ₂	2	E	IR spectra, vib. dissociation	NB, IR laser	M8403
NH ₃	2	E	vib. dissociation	NB, CO ₂ laser	M8404
HF	2	E	vib./rot. dissociation	NB, IR laser, MW	M8405
NH ₃	2	C	photo-ionization energy	RHF	M8406
HCl	2	E	rot. spectra	cell, IR laser	M8407
HF	2	E	RF/MW spectra	NB, RF, MW	M8408
NH ₃	2	C	structure	CISCF	M8409
He·Br ₂		E	rot. structure	NB	M8410
HO ₂	2	C	structure	SCF	M8411
NO	2	E	E-energy loss spectra	Pt substrate	M8412
HF	2	E	vib. relaxation	NB, laser	M8501
C ₂ H _n	2	E	rot. spectra	NB, IR laser	M8502
NH ₃	25>	E	proton transfer	NB, UV	M8503
HF	2	E	rot. spectra	NB, MW	M8504

Table 3 Molecular clusters (continued)

Type	Size	E/C	Subjects	Methods	Ref.
HO ₂	2	C	structure, vib.	CISCF	M8505
NH ₃	65>	E	MPI-dissociation	NB, laser	M8506
HCN	n	E	IR, FIR spectra	matrix, IR, FIR	M8601
HF	3, 4	C	dissociation	SECPP, SCF	M8602
HF	2	E	IR spectra	matrix, IR	M8603
NH ₃	2	C	E-structure	SCF	M8604
NO	2	E	vib. dissociation	NB, laser	M8605
N ₂ O	6>	E	fragmentation, PE	NB, synchrotron rad.	M8606
CO ₂	n	C	photo-evaporation	transition theory	M8607
NO	2	E	reaction (O, NO)	cross beam	M8608
C ₂ H ₄	2	C	IR spectra	SCF	M8609
Cl ₂	n	E	reaction (Ba)	OB, NB	M8610
NH ₃	2	E	structure, IE	NB, laser, EB	M8611
C ₀ O ⁺	n	E	reactivity, collision dissociation	NB	M8701
CO ₂	2	E	IR spectra	NB	M8702
CO ₂	560>	C	icosahedral structure	relaxed crystalline	M8703
C ₂ H ₄	n	E	IR spectra	NB, CO ₂ laser	M8704
CO ₂	15>	C	binding energy	reaction rate theory	M8705
NH ₃	n	E	CARS spectra	NB, CARS, Nd: YAG	M8706
NaCl	4	C	isomerization	E-localized	M8707
CO ₂	13>	C	E-affinity	E-phonon model	M8708
O ₂	2	C	E-spin	spin potential	M8709
C ₂ H ₄	5>	E	vib. dissociation	NB, CO ₂ laser	M8710
NH ₃	3	E	rot structure	NB, FTMW	M8711
N ₂	2	E	photoelectron spectra	NB, He	M8801
NH ₃	2	E	E-fragmentation	crossed beams, EB	M8802
N ₂ O	2	E	reaction (Ba)	crossed beam	M8803
N ₂ ⁺ⁿ	n	E	ionization	NB, EB	M8804
N ₂ O	2	E	IR spectra	NB, FTIR	M8805
CO ₂ ⁻	13>	E	photoelectron spectra	NB, EB, Nd: YAG	M8806
C ₆ H ₆	3	E	E-spectra	NB	M8901
CO ₂	n	C	structure, dynamics	MD	M8902
HF	n	C	size distribution	MC	M8903
CO, CO ₂	2	E	IR, MW spectra	NB, MW, IR laser	M8904
NH ₃ ⁺	n	E	structure	NB	M8905
CO	2	C	intermolecular potential	CISCF	M9001
O ₂ ⁻	n	E	photoabsorption	NB	M9002
CO ₂	2	E	-H ₂ O cluster, structure	NB	M9003
NH ₃	2, 3	C	intermolecular potential	CISCF	M9004
C ₆ H ₆	2	C	structure, dipole moment	CISCF	M9005
HCN	2	E	-CO, N ₂ , NH ₃ , H ₂ O clusters	NB	M9006

Atomic and Molecular Clusters

Table 4 Water clusters

Size	E/C	Subjects	Methods	Ref.
2	C	potential	CISCF	W7601
2	C	rot. structure	group theory	W7701
2	E	vib. structure, elec. resonance	NB, RF/MW spectra	W7702
2	E	PI=11.2eV, proton affinity	NB, laser	W7703
2	C	interaction energy	<i>ab initio</i> perturbation	W7901
2	E	rot. structure	NB, RF/MW spectra	W8001
2 ⁺	C	stability	proton motion	W8002
2	C	structure, isomer	CISCF	W8003
2 ⁺	E	reaction (O ₂)	ion drift tube	W8004
8	C	phase transition, energy	polarization model	W8005
2	C	interaction energy	3 config. perturbation	W8201
5>	E	vib. structure, interact. energy	NB, IR spectra	W8202
2000	E	size distribution	NB, 2nd ion detect.	W8203
6>	C	formation energy	metro. MC	W8301
2	C	interaction energy	HFSCF	W8302
2	C	vib. structure	HFSCF	W8303
200>	E	structure	NB, E-diffraction	W8304
8 ⁻	C	energy	HFSCF	W8401
8>	C	structure, interact. energy	HFSCF	W8402
48>	C	energy	HF	W8403
16>	E	size distribution	NB	W8404
3>	E	predissociation energy	NB, laser	W8501
2	C	potential	HFSCF	W8502
2	C	structure, energy	HFSCF	W8601
10>	E	detection	NB	W8602
2	C	interaction energy	HFSCF	W8603
2	C	vib. structure	inter-intra coupling	W8604
3>	C	e-localization, structure	MC	W8605
2	E	IR spectra	Kr matrix	W8701
2	E	CARS spectra	NB, CARS	W8702
3	E	IR spectra	Ar, Kr matrix	W8703
3, 4, 6	C	structure, energy	non-add. potential	W8704
5	C	structure, stability, 5-300K	MD	W8705
n	C	formation energy, entropy	effective Hamiltonian	W8706
2	E	rot. transition	NB, MW	W8707
1-4	C	intra-vibration	SCF	W8708
128>	C	electron localization	path integral	W8709
2	E	OH stretching	NB, matrix	W8801
5	C	properties	SCF	W8802
64, 128	C	dynamics, vib. states	MD, SCF	W8803
2	C	interaction	CISCF	W8804
n	C	melting	MD	W8805
140>	E	photo-fragmentation/detachment	NB, Nd: YAG	W8806
2	C	electron density distribution	SCF	W8807
10>	E	formation in binary mixtures	NB	W8901
2	E	IR spectra	NB	W8902
2	C	intermolecular potential	SCF	W9001
n	C	E-structure	SCF	W9002